

Zone Plate Array Lithography in the Deep UV

by

Ihsan Jahed Djomehri

B.S. Electrical Engineering and Computer Science, University of California at Berkeley, 1997
A.B. Physics, University of California at Berkeley, 1997

Submitted to the
Department of Electrical Engineering and Computer Science
in partial fulfillment of the requirements for the degree of

Master of Science

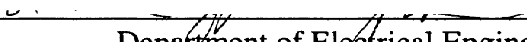
at the

Massachusetts Institute of Technology


September 1998

© 1998 Massachusetts Institute of Technology
All rights reserved

Signature of Author

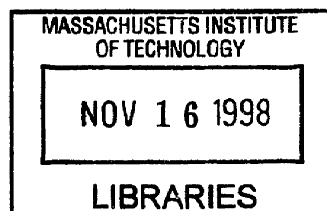

Department of Electrical Engineering and Computer Science
September 1998

Certified by


Henry I. Smith, Professor of Electrical Engineering and Computer Science
Thesis Supervisor

Accepted by


Arthur C. Smith
Chair, Department Committee on Graduate Students



ARCHIVES

Zone Plate Array Lithography in the Deep UV

by

Ihsan Jahed Djomehri

Submitted to the
Department of Electrical Engineering and Computer Science
on September 1998 in partial fulfillment of the requirements for the degree of

Master of Science

Abstract

Initial design and development of a new paradigm in nanolithography, zone plate array lithography (ZPAL), has yielded a clearer understanding of its operation, construction, and performance. The benefits of ZPAL as a maskless strategy to write arbitrary patterns with ~25 nm resolution are explored. To optimize the properties of the system required proper design of zone plate focusing. Due to ZPAL's universality, the study has been conducted in the deep UV; a process to create zone plates with 250 nm theoretical spots sizes for this regime was developed. Familiarity with nanofabrication technology proved essential, especially e-beam lithography. Next, an optical setup was built replete with alignment interferometry, precision stage motion, and radiation from a 193 nm ArF laser. A rubric for the implementation of the multiplexing coupled with coordination architecture demonstrated a potentially high throughput of $1 \text{ cm}^2 / \text{s}$. Moreover, the results of exposure tests show digital pattern generation from an array of beamlets. Because the ideal ZPAL system would function with x-rays, a discussion on its design and practical development has been included. Despite anticipated hurdles, spearheading this venture promises to drive lithography to its limit.

Thesis Supervisor: Henry I. Smith

Title: Professor of Electrical Engineering and Computer Science

Acknowledgements

The project reported on in this paper is the culmination of a year's efforts of research in the field of lithography that was made possible by the mentorship and generous assistance of a number of colleagues at M. I. T.'s NanoStructures Laboratory. The tutelage and guidance of Professor Henry Smith has proven essential in carrying ZPAL out of its infancy. I am deeply appreciative of the support that has been granted to me to complete this thesis. My gratitude also includes, but is not limited to, the helpfulness of Tim Savas especially, Juan Ferrera, James Goodberlet, David Carter, Dario Gil, and staff members Mark Mondol and Jim Daley. I am honored to have worked with such a talented group and look forward to further collaboration.

Table of Contents

Introduction	7
1 Theory and Design of ZPAL	9
1.1 Why ZPAL?	
1.2 Overview of Maskless Strategy	
1.3 Design of Zone Plates	
2 Nanofabrication Technology	19
2.1 Processing DUV Zone Plates	
2.2 Electron Beam Lithography	
2.3 Microscopy of Nanostructures	
3 Building a DUV ZPAL System	27
3.1 Configuration of Experiment	
3.2 Interferometry for Alignment	
3.3 Laser Radiation	
4 Using the Exposure System	33
4.1 Multiplexing Operation	
4.2 Coordination for Exposure	
4.3 Digital Pattern Generation	
5 Future Focus of ZPAL	39
5.1 Design of an Ideal ZPAL System	
5.2 Developing X-Ray ZPAL	
5.3 Conclusions	
Appendix	45
References	47

Introduction

This thesis seeks both to describe and to provide a working knowledge for preliminary experimental research into developing zone plate array lithography (ZPAL), a technique capable of extending the lithographic process to its limits. In anticipation of the constant miniaturization of integrated devices, ZPAL's goal is to utilize short wavelength radiation to produce the small feature sizes necessary for the realization of nanotechnology.

Chapter 1 elaborates on the theoretical motivations and functionality of the ZPAL project and outlines the design of such a system. The discussion covers the general strategy for maskless pattern generation, from considerations of radiation source to pixel focusing elements, to multiplexing and stage coordination. Furthermore, a review of the principles of diffraction and a tutorial on zone plate optics lay the foundation for the optimization of this technique to fit desired system parameters and budgets.

Chapter 2 deals with the fabrication challenges involved in producing and characterizing nanostructures. In particular, the lithography steps, associated laboratory tasks and equipment required to process DUV zone plates as vital components for ZPAL are revealed. Because electron beam lithography plays the critical role in pattern definition, its mechanism and features receive closer inspection. Finally, various methods of microscopy in the nanoscale regime depict the qualities of the structures.

Chapter 3 details the experimental setup and operation of the optical modules in a ZPAL system designed to operate in the deep UV. An overview of the configuration traces the beam paths through the alignment, control, and exposure optics and recounts their assembly. Next, a

procedure for the alignment of the zone plate array with the stage utilizing techniques in interferometry is presented. Also, a treatment of laser radiation shows its practical usage as a coherent source of illumination.

Chapter 4 expands on the intricacies of the exposure system and evaluates the results of a ZPAL demonstration. An analysis of the ideal multiplexing strategy and predicted throughput offers its feasibility, while an explanation of the algorithm for coordination of the stage motion with multiplexing illustrates how patterns form. Most importantly, the accomplishment of the digital exposure of an array of arbitrary geometries supports the development of this novel technology.

Chapter 5 summarizes the concepts of ZPAL and applies them to a future system that stands as an aesthetically pleasing candidate for sub-100 nm lithography. Thus, calculations are presented for the performance and design of ideal ZPAL. Moreover, the aspects of this x-ray ZPAL including fabrication and setup considerations parallel the discussion of the DUV case. To conclude, commentary expounds upon the relevance of the thesis work, issues and hurdles to overcome, and possible future paths of research.

1 Theory and Design of ZPAL

1.1 Why ZPAL?

The concept of a nanolithography system comprised of a short wavelength radiation source, an array of Fresnel zone plates and a multiplexing element has been proposed earlier as a means to achieve 25 nm resolution in thick resist [1]. Consequently, there are many virtues in this ZPAL technique that demand inspection.

Current methods of optical projection lithography require the use of a mask that acts as a stencil through which incident radiation exposes a specified pattern in resist. Industry widely expects to feel the burden of the rising costs of mask fabrication. On the other hand, the nature of ZPAL promises simple, non-contact maskless writing using zone plate array structures with excellent focusing characteristics.

Yet another attractive aspect of ZPAL manifests itself in its ability to pattern arbitrary geometries with multiple beamlets. Each zone plate assumes responsibility for exposing pixel by pixel a unique shape determined by its own particular multiplexing sequence. Thus, the strategy exhibits similarity to dot matrix printing and effectively digitally creates the desired image with high accuracy. Introducing a gray scale into the pixel exposure times can even achieve finer resolution due to levels of pixel overlap.

Because ZPAL is scalable, minimum feature sizes can shrink anywhere from conventional linewidths to the lithographic limits; hence, this technology offers a means of manufacturing nanodevices. By proper design, the resolution of the zone plates will be limited to their outermost zone width (written with an electron beam) and half the wavelength of the incident radiation.

An interesting feature of zone plates is their applicability to both photons and other particles of any De Broglie wavelength. For instance, free-standing zone plates for use with particles have been fabricated [2] and could be used as another focusing method in neutral atom beam lithography [3]. The ideal radiation for nanolithography, however, would be the 4.5 nm x-ray, known to exhibit no proximity effect [1].

In light of the flexibility of the ZPAL principle, the decision was made to pursue development using the deep UV radiation from an ArF laser with the 193 nm line since an x-ray source was not readily available. This choice provides the opportunity to probe the strengths and weakness of the system.

1.2 Overview of Maskless Strategy

To fully understand the workings of ZPAL, one must examine each component at a time and familiarize oneself with the procedure for coordinating them for writing. Moreover, an analogue of this analysis remains valid for any form of maskless lithography. In general, the lithography system consists of an exposure source, an array of elements that generate pixels, a method of selecting certain pixels to fire, stages to scan the cells where the patterns form, and any extra equipment for alignment or support.

The requirement on the incident radiation for maskless lithography is primarily that it have sufficient intensity to expose the resist. When using zone plates, to avoid chromatic aberration implies a narrow source bandwidth and the number of zones (hence the number of waves summed smoothly at the focus) is limited to the inverse of this bandwidth [1]. Additionally, the spatial coherence of the radiation wavefront over each focusing unit is critical to its operation.

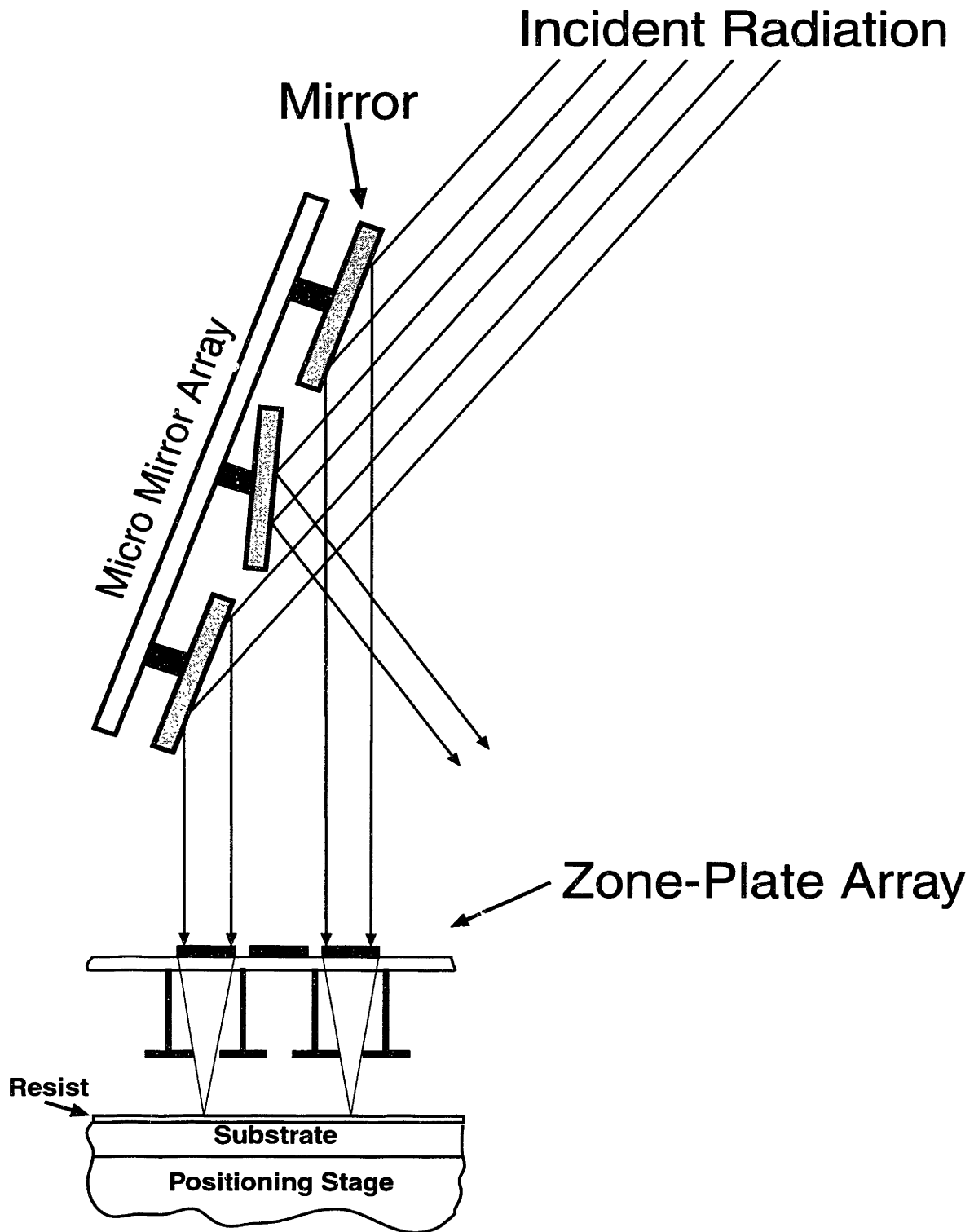


Figure 1: Diagram of a ZPAL system using a micromirror array to multiplex incident radiation onto a zone plate array that exposes a substrate.

Probably the best location for the multiplexing capability lies just upstream of the focusing array so as not to interfere with the substrate. In order to physically turn on or off each individual beamlet, an array of micromechanical devices can be employed. Also, the multiplexing must have a fast addressing scheme similar to those used in active matrix displays. As an example, Figure 1 proposes a schematic of a ZPAL system that employs an array of micromirrors that pivot to deflect the incident radiation into or away from the zone plate array. Another method of multiplexing utilizes micromechanical shutters to block each beamlet.

The uniqueness of any maskless lithography concept reveals itself in the manner in which pixels are generated. One can imagine the Fresnel zone plate as the lensing optics needed for short wavelength particles. From the principles of diffraction theory, radiation impinging on a grating will deflect into various orders; hence, a zone plate is a circularly symmetric grating with the period ramped such that the first order of the inner and outer zones share a common focus.

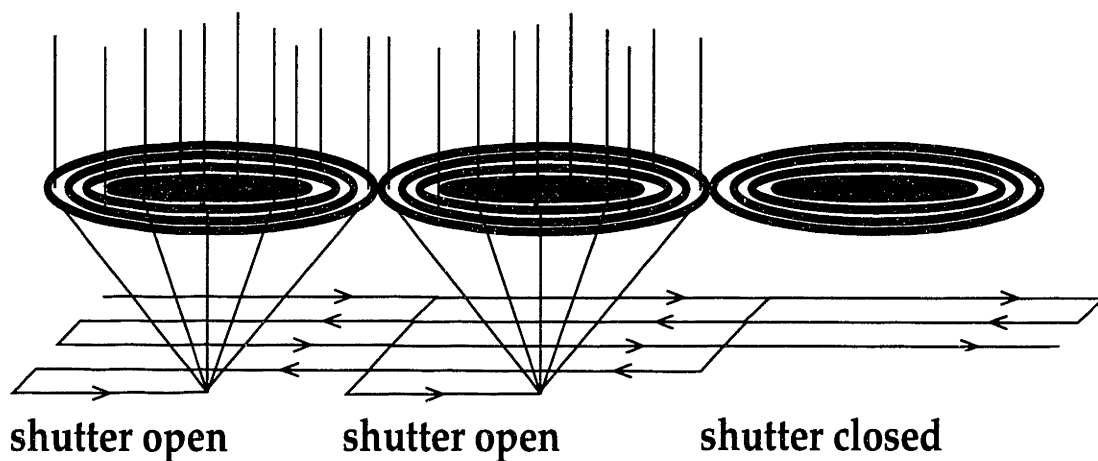


Figure 2: Representation of a coordinated maskless writing strategy in ZPAL. The stage scans while the multiplexing unit selects which zone plates shall expose pixels.

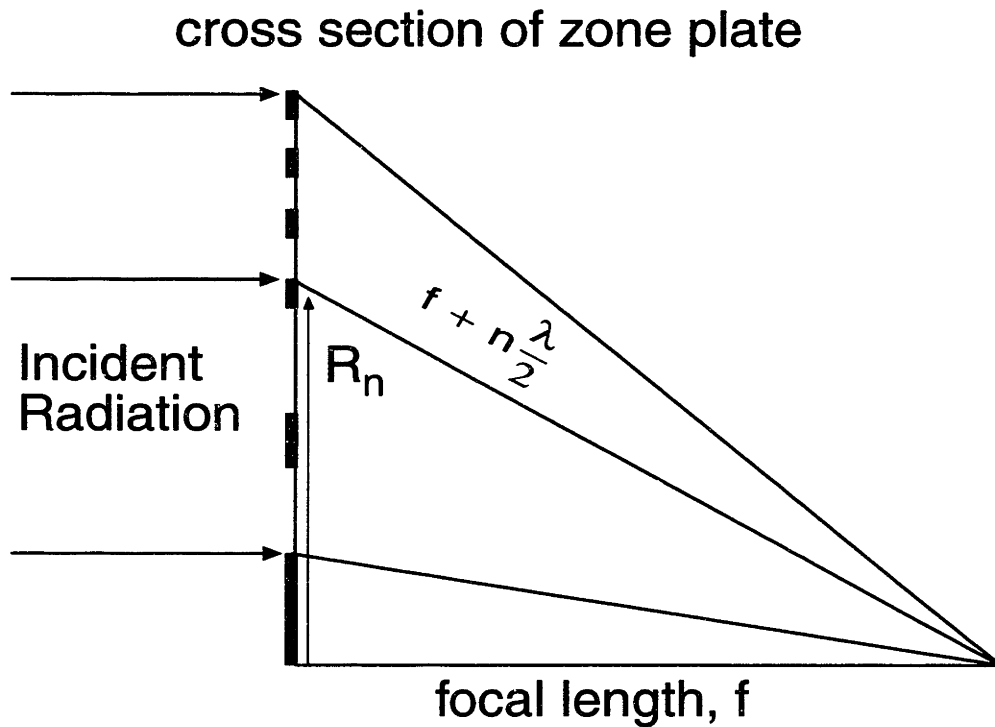
Precision control of the stage motion ties together all the modules of ZPAL to produce a planar, digital image. Many possible scan modes exist, but each must ensure stage translation in pixel diameter steps within a time on the order of the spot exposure time for highest throughput. Figure 2 endorses a serpentine writing scheme where the stage scans back and forth, skipping down a row in the cell at the end of the current row, and each zone plate exposes the line underneath its own cell as long as it remains in the multiplexed on state.

1.3 Design of Zone Plates

The principles of diffraction applied to zone plate structures give formulas for deducing the focusing characteristics based on certain design parameters. Also, by choosing the attenuation and phase relation (not always separable due to the material) between adjacent zones, the efficiency in a particular order is calculated and determines the contrast between pixels and the background dose.

In fact, there are few independent variables to choose from to influence the zone plate. Essentially, one selects a certain wavelength of radiation, λ , that satisfies the intrinsic resolution requirements of the system. Second, the total number of zones, N , in the zone plate is fixed according to the source bandwidth, BW , and the desired size. Finally, the outer zone period, p (theoretically twice the diffraction limited spot size), sets the most conspicuous figure of merit.

Given a set of system parameters, one derives several optical properties of the zone plates. With reference to Figure 3, each zone radius, R_n , forms a Pythagorean triangle with the focal distance, f , as a base and f plus an integral number of half wavelengths as the hypotenuse. This



$$R_n^2 + f^2 = \left(f + n \frac{\lambda}{2} \right)^2$$

Figure 3: Illustration of the relationship between the important quantities in zone plate design: focal length and zone radius.

condition ensures that every other zone inputs the same phase at the focus, effectively creating a chirp for the zone radii. Rearranging,

$$R_n = \sqrt{n \cdot \lambda \cdot f + \frac{n^2 \cdot \lambda^2}{4}} \quad (\text{Equation 1})$$

Since one has chosen an outer zone width which must then equal to $R_N - R_{N-1}$, one can proceed with a non-linear solution of focal length. An iterative solver for this equation has been programmed in C, and Figure 4 renders the three dimensional surface of design possibilities.

Using the computed value for f , the radius of the zone plate, R_N , is then found by substitution.

Thus, the overall area of the zone plate and its gap to the substrate become known properties. The depth of focus, important in delineating the minimum error in focal distance, can be defined as the distance in which the beam waist doubles. By simple geometry,

$$DoF = \frac{p}{2} \cdot \frac{f}{R_N} \quad (\text{Equation 2})$$

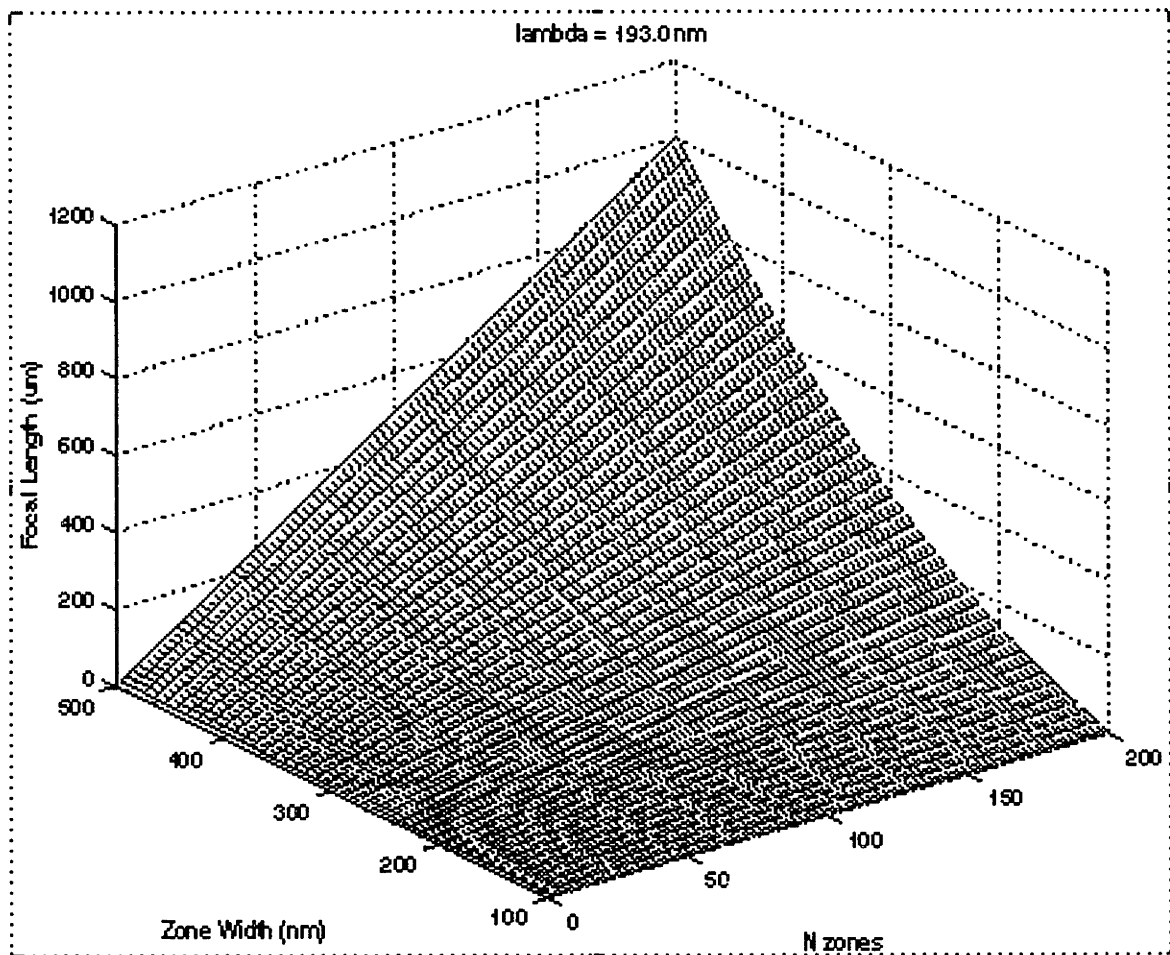


Figure 4: Plot of possible zone plate design focal lengths by specifying the wavelength, outer zone width, and number of zones. Generated in Matlab.

For the purposes of the DUV zone plates as shown in Figure 5, materials of a real-valued index of refraction (i.e., no attenuation) are available. This circumstance leads to the ability to fabricate a pure phase zone plate rather than the common amplitude zone plate with every other zone fully blocked. By introducing a π phase shift between adjacent zones, the zero-order radiation is totally cut off while the first-order focus receives 40% of the radiation incident on the zone plate [4]. In contrast, the amplitude zone plate offers only 10% efficiency to the focus and 25% to the zero order. Blazing the zones would further increase the efficiency; however, the technique presents processing complexity.

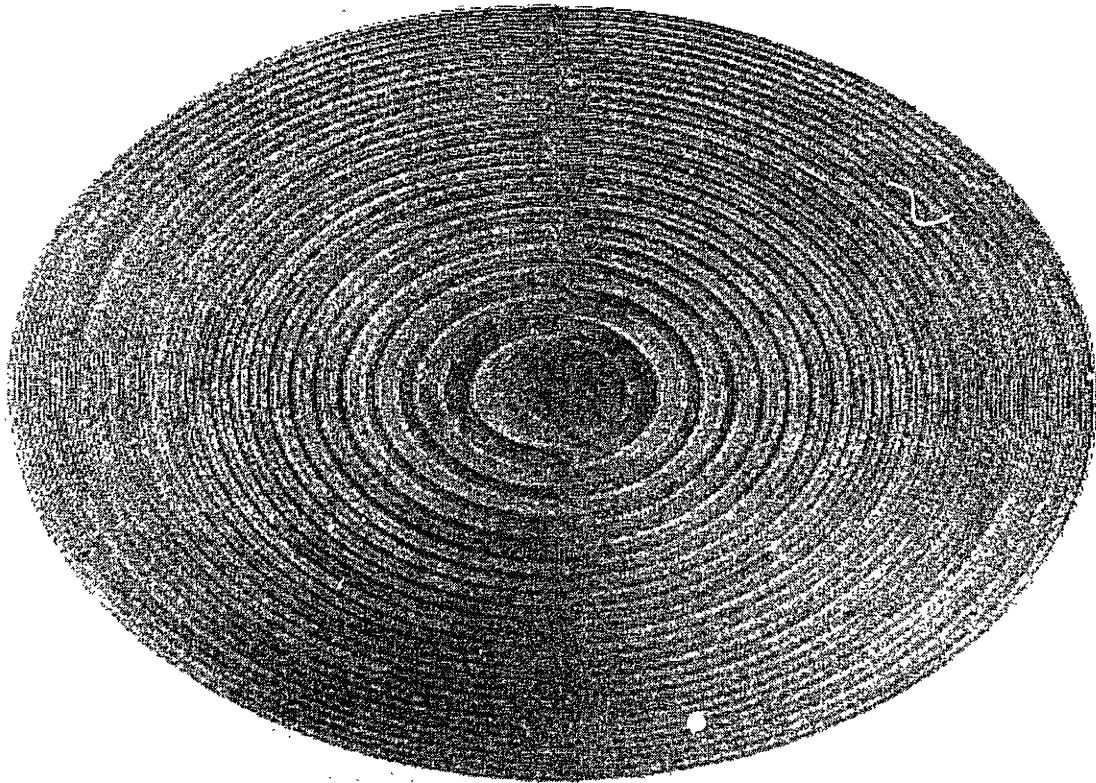


Figure 5: Scanning electron micrograph of a pure phase DUV zone plate.

At all times, contrast in the resist between the pixel dose and background radiation should remain high. Specifically, the ratio of first order to cumulative other order efficiency must exceed the ratio of the area of the focal spot to the zone plate area multiplied by the number of pixels per cell (since the background affects the entire cell):

$$\frac{\epsilon_1}{\epsilon_{other}} > \frac{A_{spot}}{A_{ZP}} \cdot pixels \quad (\text{Equation 3})$$

Because the development rate in PMMA exhibits an approximate cubic dependence on dose, a 2:1 contrast is acceptable, although higher contrast is certainly desirable.

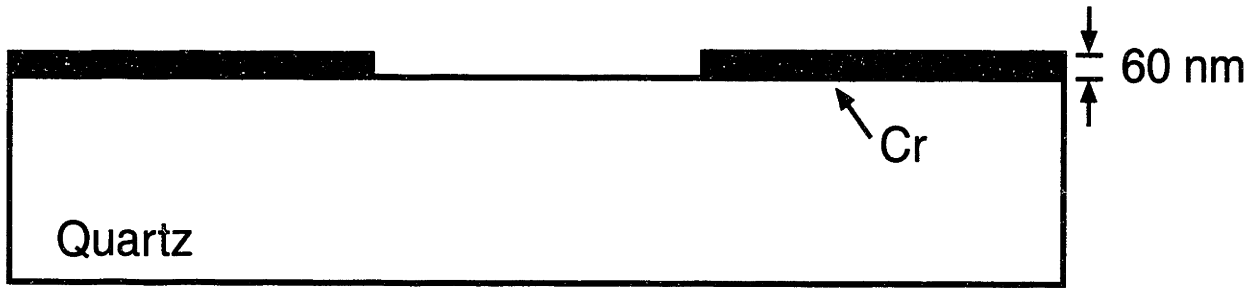
2 Nanofabrication Technology

2.1 Processing DUV Zone Plates

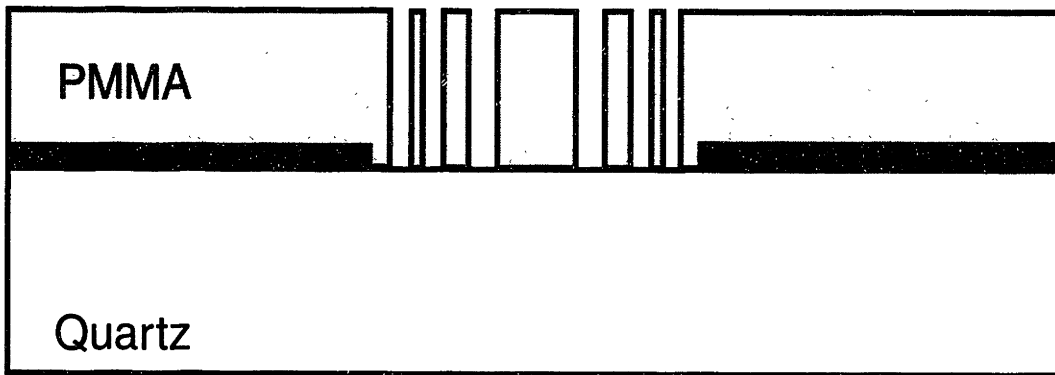
One of the most challenging tasks in developing the deep UV ZPAL system appears as the fabrication of the small featured phase zone plates. Therefore, a discussion of modern sub-micron processing techniques is called for. For experimental purposes, arrays of zone plates were created with 50 zones having respectively theoretical spot sizes of 250 nm and 500 nm, radii of 24 μm and 49 μm , focal lengths of 57 μm and 249 μm , and depths of focus 0.6 μm and 2.5 μm . Figure 6 provides a flow of the process cross-sections through the lithography and etch steps.

To begin, the choice of substrate for the zone plates must exhibit transparency at the selected 193 nm DUV, and must possess optical flatness (e.g., $\lambda / 100$) over the array: a quartz wafer satisfies these conditions. Next, one wishes to coat what will be the intervening space between zone plates with metal to block excess radiation. An evaporation of 60 nm of chromium on the quartz provides several skin depths of attenuation (calculated from the complex index of refraction of Cr). Then, an e-beam lithography step defines regions of metal to strip away as well as alignment marks for the second step. After developing the PMMA resist, a standard chemical wet etch of Cr followed by PMMA stripping in an oxygen plasma asher leaves the wafer ready to define the zone plates.

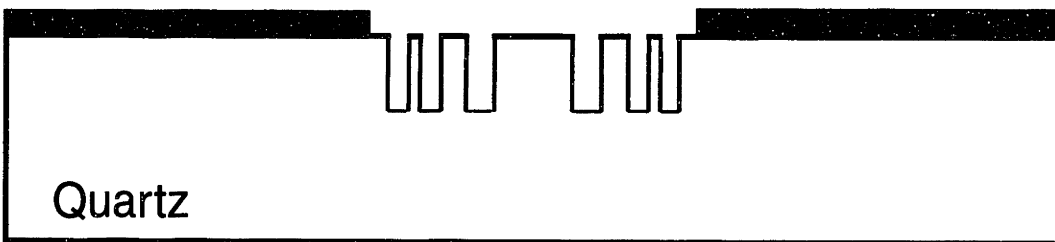
The procedure for achieving the fine zone plate features relies on electron-beam exposure and pattern transfer using “dry” reactive ion etching. Because PMMA exposure results in chain scission and development rate is a strong function of polymer length, high resolution can be obtained. First, the 300 nm thick (to serve as an etch mask) PMMA coated wafer undergoes field



Pattern chrome on quartz.



E-beam expose and develop zone plate in PMMA.



CHF₃ RIE and remove PMMA.

Figure 6: Process steps in the fabrication of DUV zone plates: patterning Cr, e-beam exposure of zone plates, RIE into quartz.

calibration and alignment in the e-beam system to ensure pattern scale and placement accuracy. Next, special software writes a sequence of true annuli (representing every other zone) to form the zones plates, one per field. After development, pattern transfer occurs via RIE in CHF_3 gas, commonly used for oxide etching. The reactive etch process involves chemisorption of the gas on the substrate, rearrangement of the surface molecule into a volatile species, and desorption [5], while ion bombardment is responsible for the vertical etch anisotropy. Because one desires a π phase difference between zones, the proper etch depth of 171 nm results from π divided by the difference in wavenumber from quartz to air, Δk .

2.2 Electron Beam Lithography

Although relatively slow, the electron beam system offers a reliable means of defining crucial small features for many applications. For the ZPAL project, a VS-2A e-beam writer was used to pattern the zones. Since e-beam quality indirectly determines the resolution capability of the zone plates, one must understand the principles behind the implementation of scanning electron beam lithography (SEBL), its dose delivery scheme, and its write strategy.

Examination of Figure 7 reveals an example SEBL system with the fundamental electron optics [5]. The brightness, B , of electrons emitted by the gun depends on the type of source used. Next, the anode plate at high voltage (e.g., 50 kV) accelerates the charged particles and sets their energy. The important relations to recall from quantum mechanics to derive the wavelength are:

$$\lambda = \frac{h}{p}, E = \frac{p^2}{2m} \quad (\text{Equation 4})$$

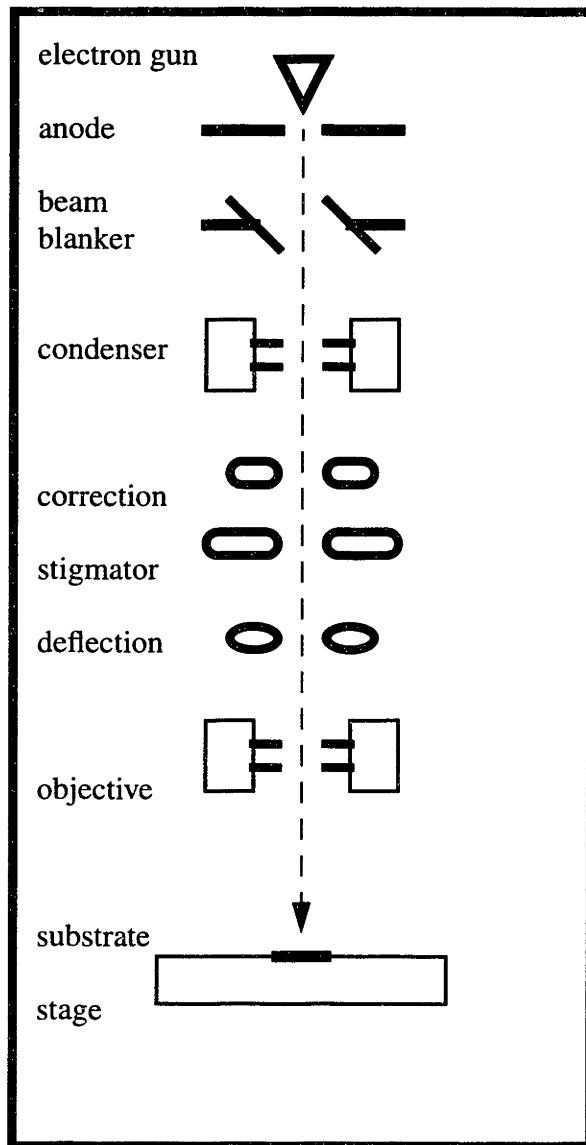


Figure 7: Schematic of a column of an electron beam system including various electron-optical components such as lenses and coils.

where p is the momentum and E is the energy. A beam blanker then shuts the beam on or off as desired via electrostatic deflection. Now the beam passes through a series of electron optics, including a condenser lens, correction coils for fine shift, stigmator coils for beam symmetry, deflection coils to write, and an objective lens. These elements act by the Lorentz force law and either have 1) plates producing an electrostatic bending or 2) coils producing a magnetic field that focuses and rotates the electron trajectory. In practice the minimum obtainable beam diameter,

$$d \propto (i/B)^{1/2} \cdot \alpha^{-1} \quad \text{(Equation 5)}$$

where i is the beam current and α signifies the maximum angular divergence of the beam (on the order of 10^{-3} rad to ensure paraxial ray assumptions). Last, the sample is mounted on a translation stage with laser interferometer control.

Like most laboratory procedures, finding the correct exposure dose requires iteration. First, a quick calculation of the dose in charge per area using the resist sensitivity yields a starting value for a dose matrix. Choosing the field size and then varying the beam current or exposure frequency factors scales the dose. To measure the current, one utilizes a Faraday cup possessing a deep hole that captures all the electrons in the beam path.

With a computer control, the user can select or create numerous write modes. In order to achieve high speed writing capability, one must program a primitive shape code for the particular feature, such as a circle to draw the zone plates. The front end software to create the zone plate pattern file is attached in the Appendix; an assembly language interface decodes this file and communicates with the beam deflection unit. Additionally, the SEBL system's electron detector images alignment marks to calibrate the field size and prepare for writing. Figure 8 displays a

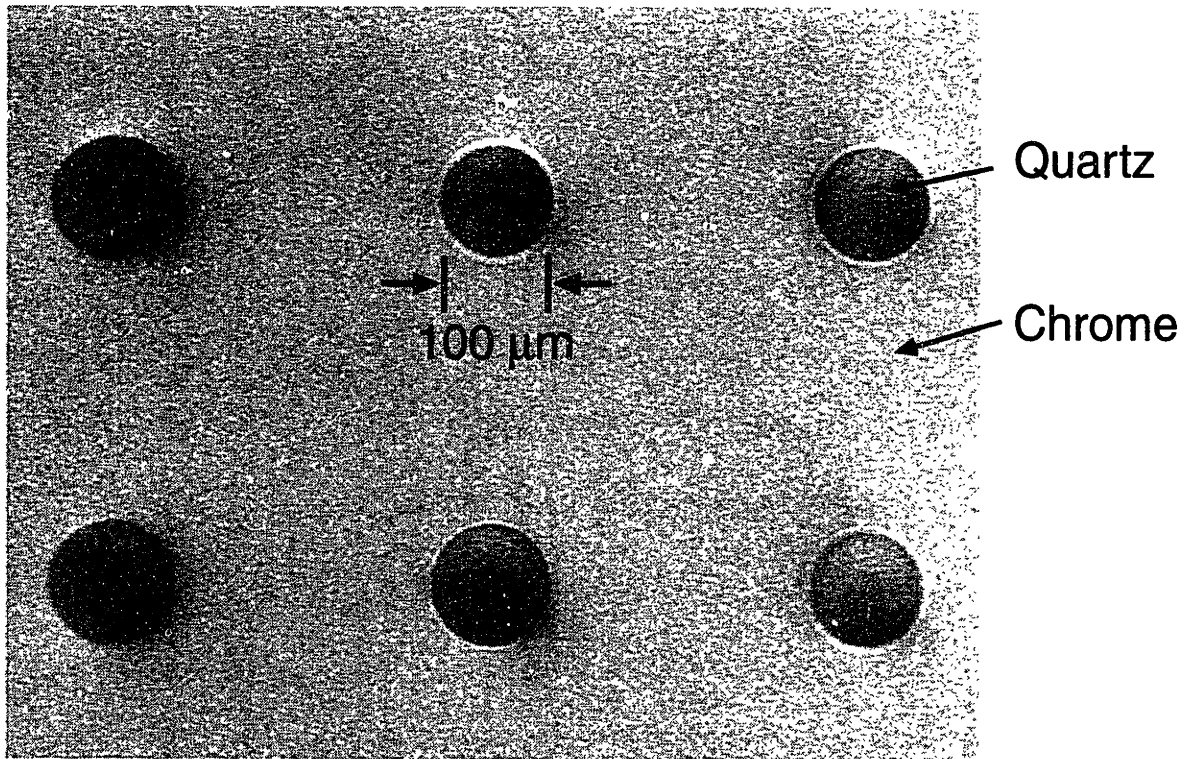


Figure 8: Scanning electron micrograph of a 2 by 3 array of zone plates etched into quartz, fabricated using aligned SEBL.

final array of zone plates that were aligned and written using SEBL. The current technology presents the problem that alignment between fields has stitching errors. However, the concept of spatial phase locking (SPL), in which a global grid on the resist provides a reference, hopes to remedy it [6].

2.3 Microscopy of Nanostructures

Characterizing the features of nanostructures often requires non-optical microscopy tools. Therefore, one evaluates the fabrication process based on a knowledge of the benefits and limitations of these systems. The popular scanning electron microscope (SEM) offers excellent

resolution with various signals, but certain aberrations must be avoided. Also, an atomic force microscope (AFM) scans images by surface probing.

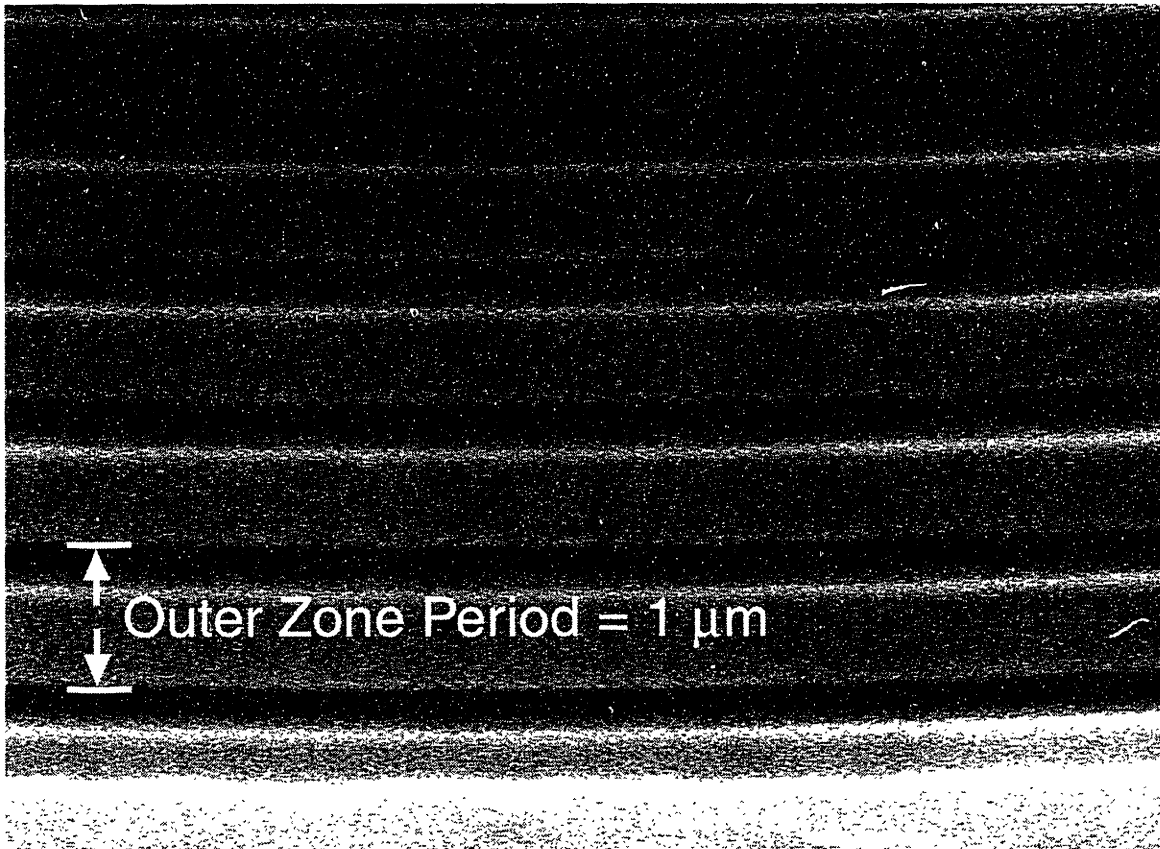


Figure 9: Scanning electron micrograph of the outermost zones of a DUV zone plate with a micron outer zone period; the SEM resolution is excellent.

Basically, the SEM operates with the same electron optical column as SEBL, but emphasizes recovery and detailed reconstruction of the signal (see the micrograph of Figure 9). Frequently used signals include high energy backscattered electrons, low energy secondary electrons (excited by the incident flux and exiting the substrate), and other radiation characteristic of the material. Image quality of the SEM is determined by the effective beam diameters of all

limitations summed in quadrature. Aberrations are dependent on α^3 for spherical, energy bandwidth and α for chromatic [7]. The diffraction limited spot of wavelength divided by numerical aperture goes as the inverse of α .

Another technique for probing surface information employs the AFM. Essentially, a tip of several nanometers radius of curvature scans the substrate, revealing the profile via a particular force mode. The image is a convolution of sample features and tip shape, as depicted in the false sidewall slopes of the zones in Figure 10.

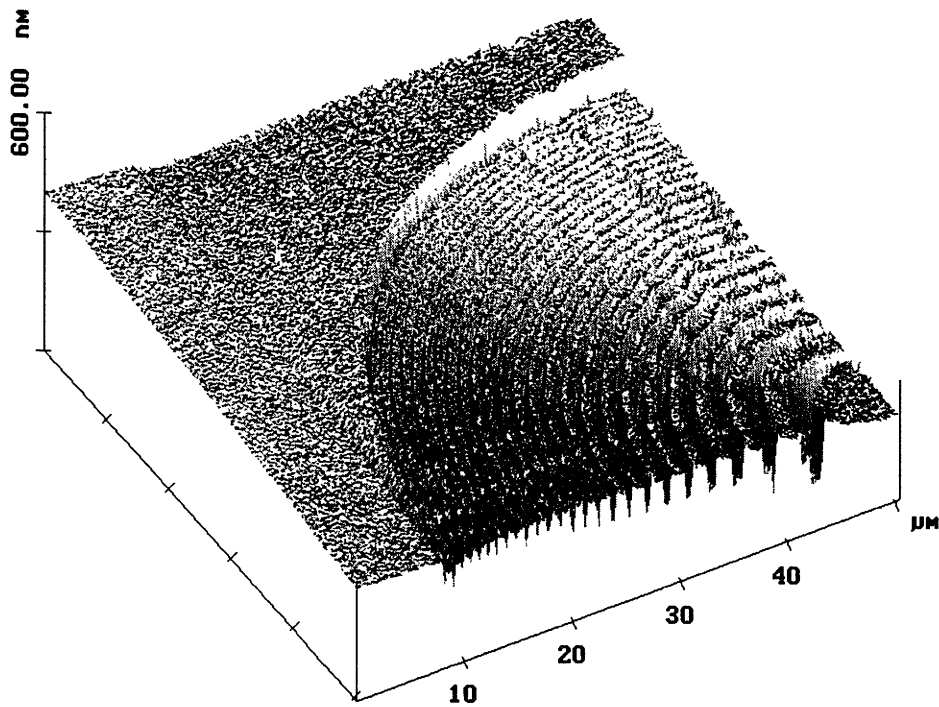


Figure 10: Atomic force microscope image of a quarter section of a 49 μm radius DUV zone plate etched into quartz.

3 Building a DUV ZPAL System

3.1 Configuration of Experiment

Preparing for a demonstration of ZPAL in the deep UV demands construction of an optical setup according to the aforementioned design. By tracking the beam paths of all light sources in the schematic of Figure 11, the relevant alignment, control, and exposure modules and their parts can be studied. The system rests on a vibration isolated optical table.

Beginning with the visible class III HeNe laser, the $\sim 1 \text{ mm}^2$ beam goes through an expander diverging lens. Almost its focal length away, a converging lens collimates the wide laser beam which is then sent into an interferometer in the Michelson configuration. A beam splitter cube partitions the beam, sending one ray to an aluminum metal reference mirror and another to the test surfaces (both the Cr face of the zone plate array wafer and the resist coated substrate). Upon reflection, the reference and test signals return and recombine in the splitter cube, producing an interference pattern that represents the degree of parallelization of the reflecting surfaces.

Sharing the same interferometer, one employs the white light source for gap alignment. Many light wave modes travel down and emerge from the optical fiber, which are subsequently converged to focus on a pinhole aperture (allowing for spatial filtering) and then collimated. The interference fringes would appear as shown opposite the reference mirror.

Radiation from an ArF laser constitutes the exposure dose. After passing through optional polarizers or attenuators, the DUV reflects off a dielectric mirror, placed below but transparent to the interferometer, at a specific angle and falls incident onto the mounted zone plate array. As a result, the zone plates diffract the radiation and expose the resist at their focal points. To control

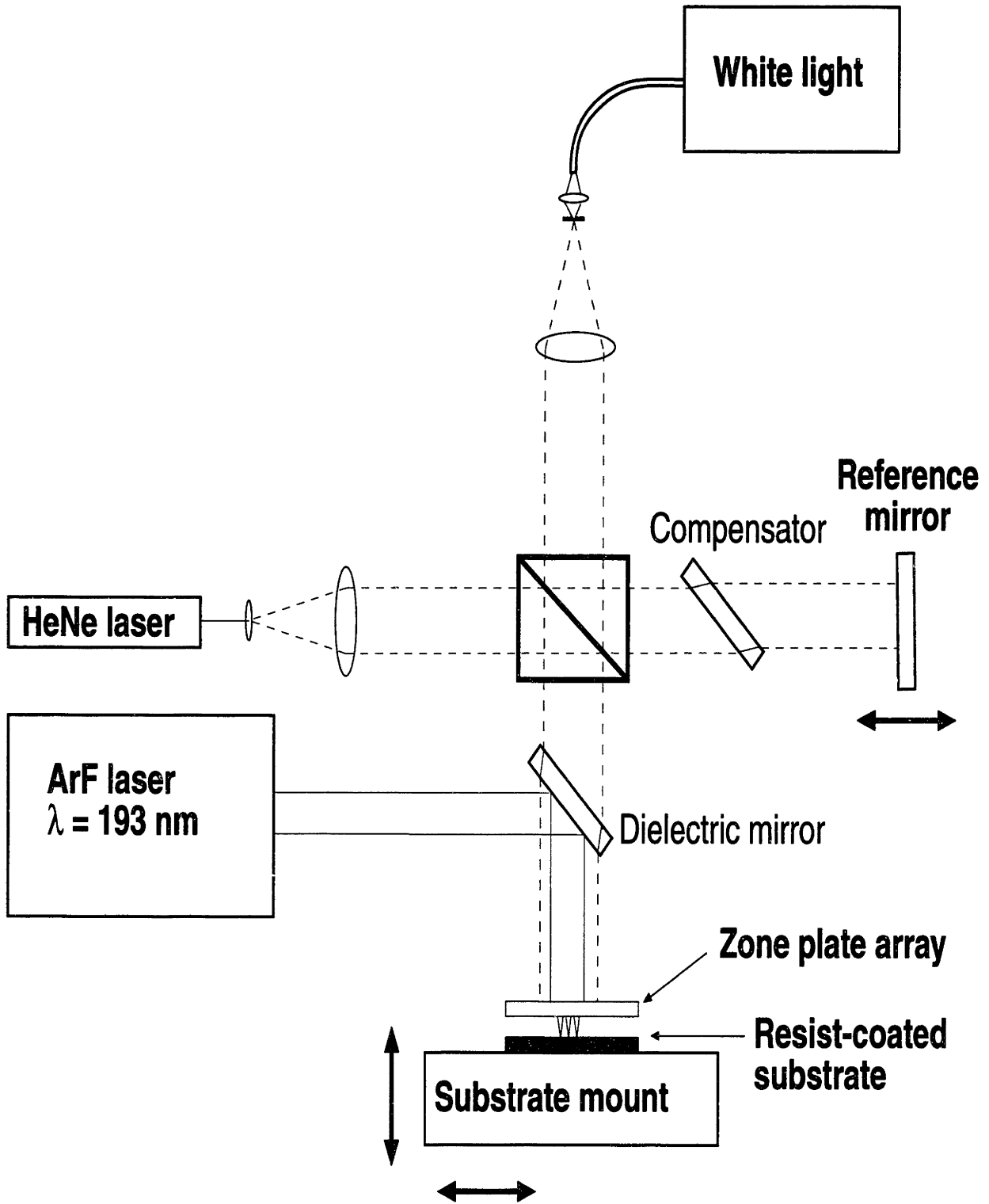


Figure 11: Schematic of the experimental setup of a DUV ZPAL system including the alignment interferometry, control and exposure optics.

the alignment and exposure routines, the substrate mount is outfitted with crossed-roller bearing stages for translation in X-Y-Z, and the reference mirror possesses a unidirectional stage. Micrometers and piezoelectric blocks on the stages enable precision travel.

3.2 Interferometry for Alignment

Because the depth of focus in ZPAL ranges on the order of a micron, a sophisticated technique must be utilized for moving the substrate into that range while parallel to the zone plate array. This accomplishment has been performed with a combination of laser and white light interferometry, as the results of a through focus test indicate.

The properties of the Michelson interferometer are well known [8] and are used for coarse alignment and parallelization. In this case, the 632.8 nm HeNe source with greater than 10 cm coherence length produces interference between the reference mirror and both the zone plate array and the substrate. By tweaking the mirror mounts, one verifies that both sets of fringes are centered, implying that the array is parallel to the substrate. When at the fringe center, one observes a large fringe surrounded by a series of co-centric fringes due to the slightly spherical wavefronts.

A procedure for the localization of the substrate at the zone plate focal distance involves the white light interferometer. By its nature, the white light emits a range of wavelengths from about 400 to 800 nm and the resulting ~900 nm coherence length comes from:

$$L_{coherence} \sim \frac{\lambda_{av}^2}{\Delta\lambda} \quad \text{(Equation 6)}$$

Hence, the two arms of the interferometer must be equal to within this length for interference fringes to form. First, one observes fringes between the reference arm and the zone plate array.

Next, one uses a sub-micron micrometer to move the reference mirror stage back by the calculated focal distance of the zone plate. The Z-stage of the substrate translates such that a detectable fringe pattern arises between the reference arm and substrate, thus placing it well within the depth of focus of the zone plates.

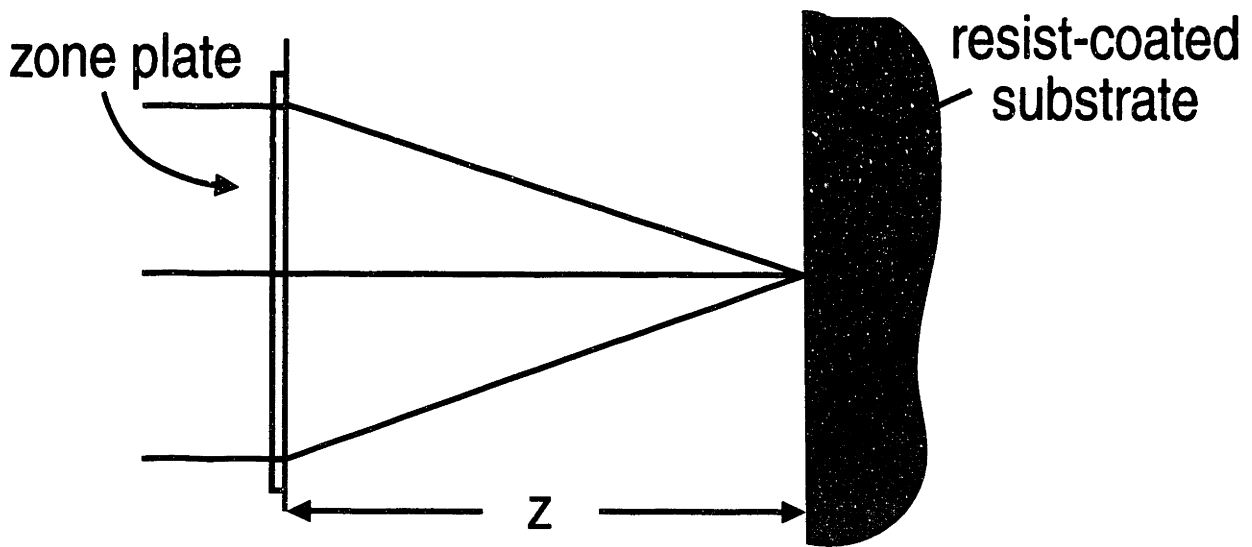


Figure 12: Diagram of a through focus experiment, depicting how moving the substrate in the direction normal to the focal plane will expose a different beam waist.

An interesting experiment to demonstrate this alignment approach follows from the cartoon in Figure 12. While incrementing the substrate stage in the Z-direction in $1 \mu\text{m}$ steps, spot exposures are taken of the beam diameter of the zone plate's first order diffraction. Clearly, Figure 13 illustrates the spot size decreasing to a minimum (indicating arrival at the focus) and then increasing again. Both the 250 nm and 500 nm outer width zone plates exhibit this trend. The fact that spots with more than twice the minimum resolution have developed implies that the dose is overexposing by a factor of at least four.

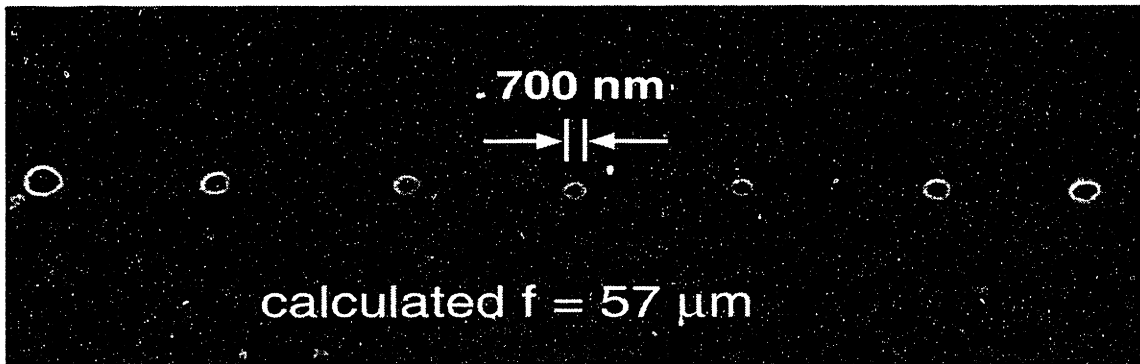
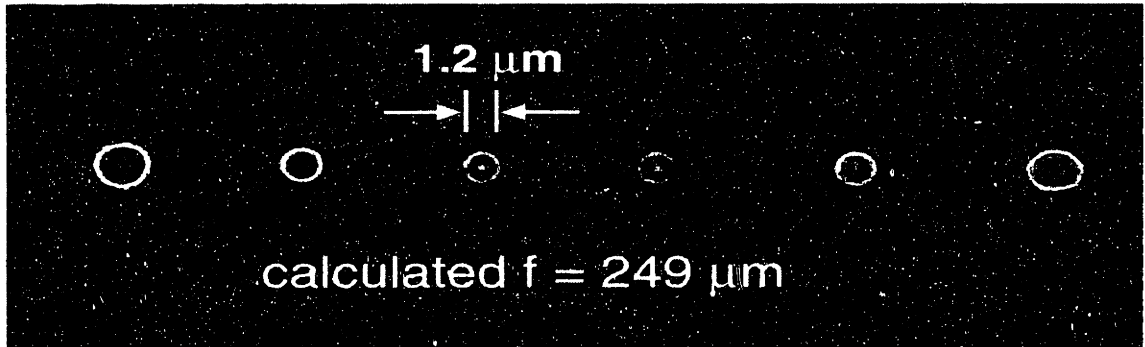


Figure 13: Scanning electron micrographs of the zone plate beam spot exposed at $1 \mu\text{m}$ increments in the z-direction and developed in PMMA. Results for zone plates of $f = 249 \mu\text{m}$ and $f = 57 \mu\text{m}$ show the spot size through the focus.

3.3 Laser Radiation

The coherence and stability of the exposing radiation assume paramount importance to the implementation of ZPAL. The physics behind laser phenomena, including specifications for the

ArF laser used, as well as the methods of manipulating this short wavelength figure prominently in the project.

The principle of light amplification by stimulated emission of radiation (LASER) plays a significant role in the quantum theory of light [9]. In a simplified analysis, an energy source (e.g., voltage on a plasma tube) pumps nearly all the electrons of a gas into a metastable energy level (slow decay time). However, when an electron falls to its ground state, it emits a photon with a characteristic wavelength that in turn stimulates another electron to fall, eventually causing a cascade of coherent radiation at that wavelength (i.e., the laser pulse).

To produce a coherent flux of deep UV radiation, an ArF laser with the 193 nm line was used. The bandwidth of about $1 / 200$ easily allows for the $N = 50$ zone plates, while collimation of 3 mrad expanded to a 1 cm^2 beam area provides sufficient illumination of the zone plate array. A drawback to the laser is that it fires in 5 to 15 mJ pulses of ~ 15 ns in duration, but repetition rates of up to 200 Hz can be set.

The difficulty in designing optics for the DUV regime lies in that many materials start absorbing the radiation very strongly. Optical windows must typically be made of some silicon oxide. To reflect the light with high efficiency requires dielectric mirrors: these are quarter wavelength thick films of alternating index of refraction designed to reflect at a certain incidence angle.

4 Using the Exposure System

4.1 Multiplexing Operation

Perhaps the most challenging aspect of the principle of ZPAL operation, multiplexing allows each zone plate to produce an individual pattern. As displayed in the downstream shuttering technique of Figure 14, the multiplexing array either keeps the pixel on or shuts off the entire radiation. The theory of the functionality of an ideal multiplexing unit is presented and compared to an available system; the evaluations result in estimates of the throughput.

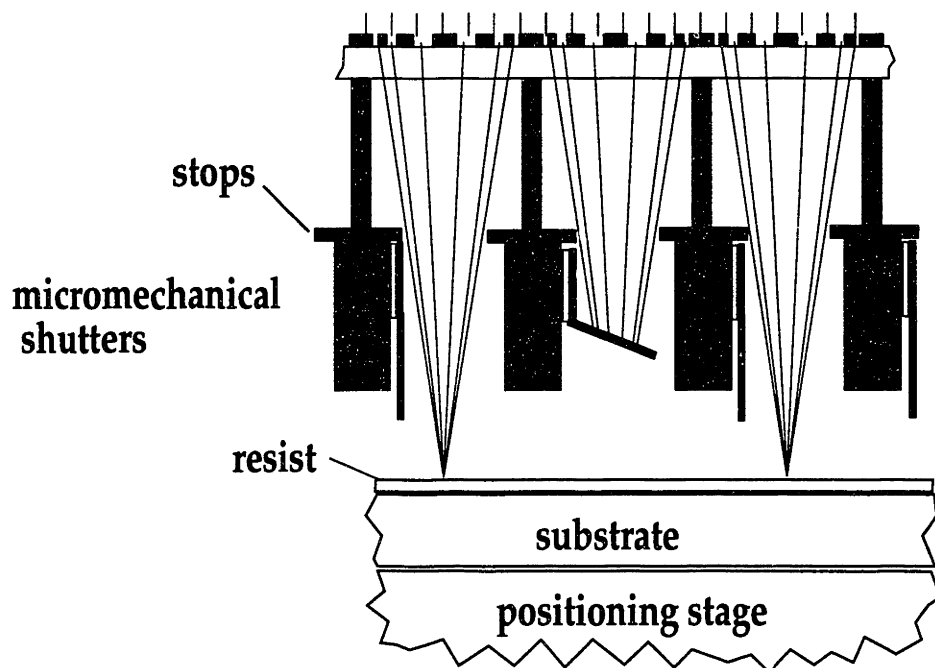


Figure 14: A multiplexing scheme using downstream micromechanical shutters to turn on or off each zone plate individually.

The architecture of a fast multiplexing system becomes vital to sustaining high data rates.

Intuitively, the condition for maximum throughput where τ represents time becomes:

$$\tau_{\text{exposure}} = \tau_{\text{frame}}$$

(Equation 7)

Here, the “frame” time refers to the time to address the entire array, permitting exposure of one pixel in each of the cells. Assuming abundant exposure flux, one must minimize the addressing time. As illustrated in Figure 15, the rows are activated in series and the columns in parallel with the proper on or off data. The total time to expose the cell is then the frame time multiplied by the number of pixels per cell, typically $\sim 10^4$. Texas Instruments has analyzed the behavior of a similar system [10].

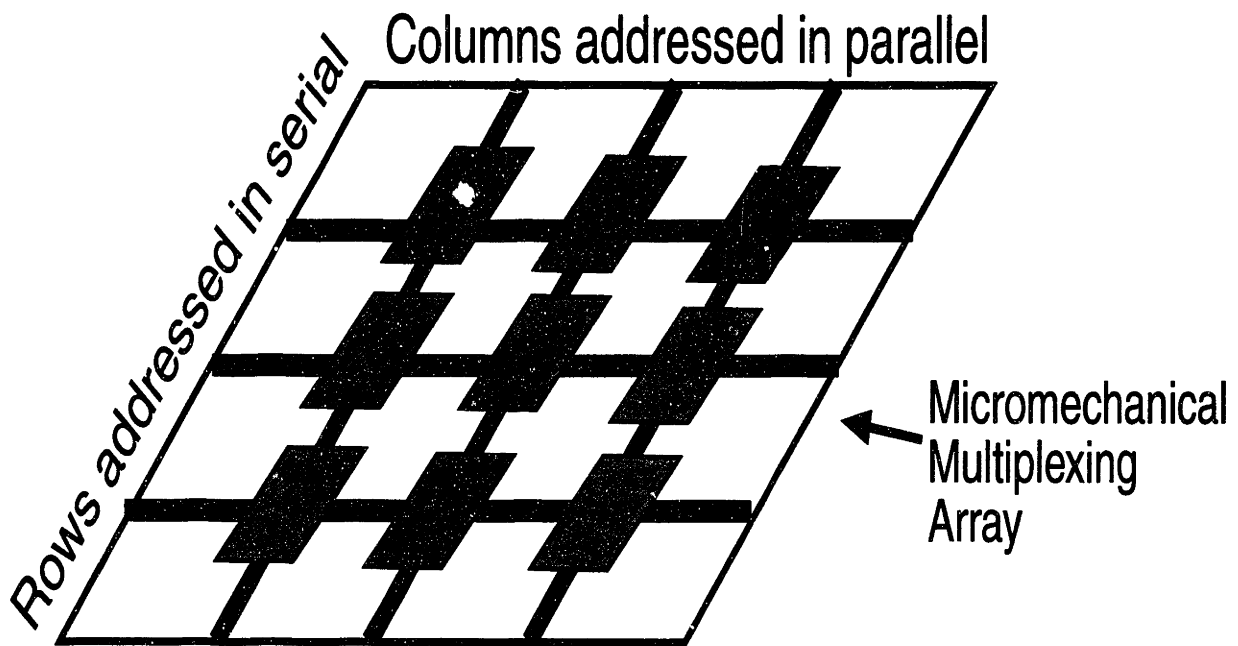


Figure 15: Illustration of a multiplexing device, a micromechanical array, in which each cell is addressed by the rows in series and the columns in parallel.

An experimentally available micromirror array system is the TI Digital Light Processing technology [11], a CMOS process compatible microelectromechanical structure (MEMS) with several hundred by several hundred aluminum coated mirrors, $16 \mu\text{m}$ to a side. An SRAM cell underneath each mirror electrostatically deflects it $\pm 10^\circ$ from on to off in a latch time less than

the frame time. If placed upstream in the beam path of incident radiation, the mirrors could deflect light in and out of the zone plates for multiplexing operation. With a frame time of about $20 \mu s$ (about 25 MHz clock rate), an entire cell could be exposed in under a second. Therefore, the throughput becomes the area covered by the zone plate array divided by this total time.

4.2 Coordination for Exposure

To properly assemble the desired pattern from computer memory into a multiplexing and stage motion sequence requires an analysis of the concept of the cell, tracing the data flow, and evaluating the drive system of the substrate translation stages.

Each pixel generating optic has full responsibility for exposing the square area directly beneath it. Defects in either the multiplexing unit, zone plate fabrication, or alignment that govern the same cell would hopefully cause only an insignificant change in exposure dose; however, isolation and abandonment of this cell by trial and error may be necessary. The stage moves constantly in a serpentine scan; every time a pixel increment is reached, a fresh frame is loaded into the multiplexing array, corresponding to the on and off values for every pixel at that cell location. Only at the end of the scan (which needs only move through the area of one cell) are the unique images in each cell complete. Because the cells are contiguous, they merge with their neighbors to form a larger pattern.

Maskless lithography implies that a large quantity of data, one bit for every pixel in every cell, must be processed and sent to the ZPAL setup. Basically, one creates a pattern layout which is then divided into a sequence of frame data that feeds into the multiplexing array for each new pixel increment. Handling this information remains one of the greatest tasks of the research.

Finally, the ideal mechanism for stage motion manifests itself in a three dimensional, computer controlled drive with laser interferometry. The accuracy of such systems are sufficient for writing ~25 nm features. In the DUV experiment, piezoelectric blocks with a more precise 100 V per micron expansion proved useful, but had small range of travel.

4.3 Digital Pattern Generation

The results of trial run exposures using the DUV ZPAL system described previously bear testimony to its sound operating principles. Analyses of the minimum features achieved, an arbitrary written pattern, and the interaction of the entire array of focusing elements all demonstrate facets of the feasibility of this technique.

Interestingly, only one 15 ns, 5 mJ pulse of the ArF laser was needed to expose the PMMA resist after focusing. The laser beam signal drops off by several factors as it propagates towards the zone plates. The ratio of the zone plate area to the beam area must be considered along with the focusing of the entire zone plate's incident flux down to one spot. Figuring from the resist sensitivity, the dose is overexposing a couple orders of magnitude. This result contributes to the 700 nm and 1.2 μ m spot sizes for the zone plates with theoretical resolutions of 250 nm and 500 nm, respectively. Another source of error in the larger than expected spots may arise due to imperfections in the line to space duty cycle of the zones.

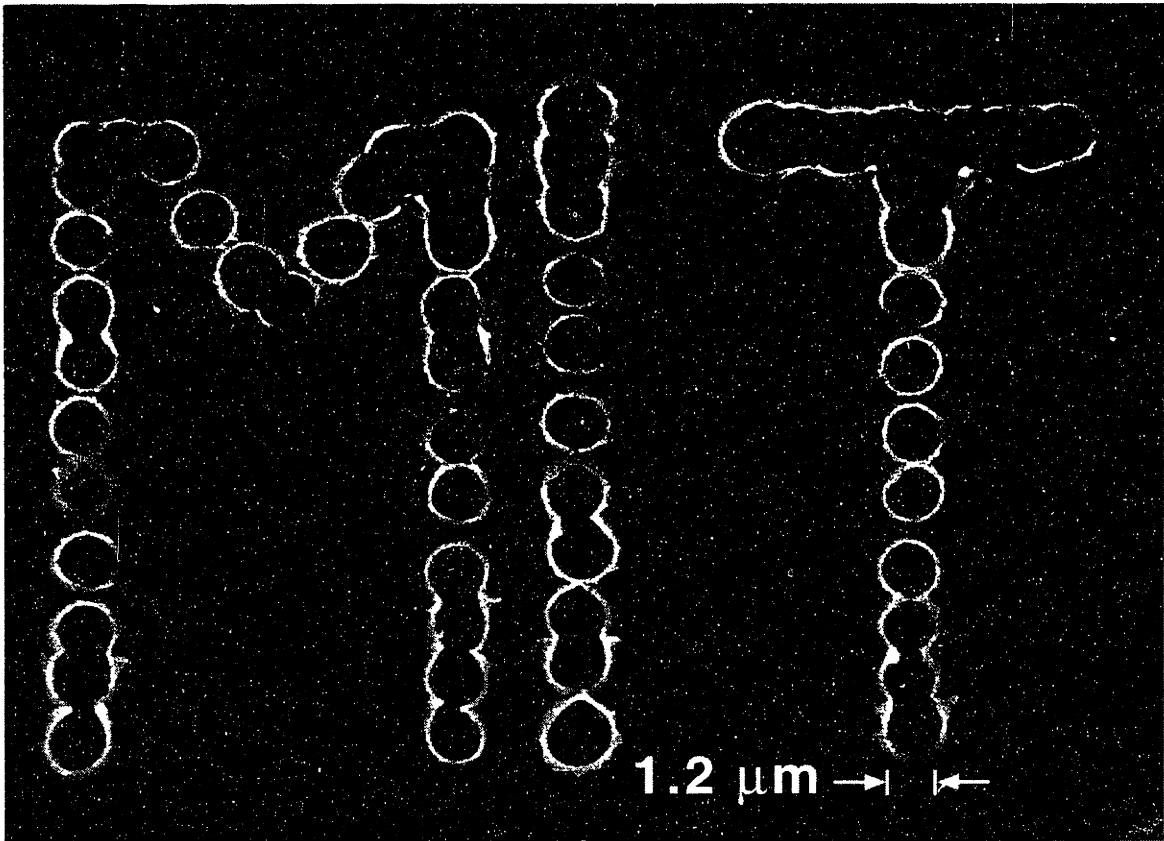


Figure 16: Scanning electron micrograph of an image, exposed and developed in PMMA, produced by ZPAL digital pattern generation.

As illustrated in Figure 16, ZPAL has created images in thick resist of a two dimensional pattern. Although the pulse by pulse exposure sequence was done by hand, a legible word "MIT" emerges. Computer controlled stage motion promises to overlap the pixels to form distinct lines. The crucial feature to recognize is that the pattern is digital in nature. Unlike errors in projection lithography, this type of pixel by pixel exposure ensures quality resolution and ease of pattern generation.



Figure 17: Scanning electron micrograph of nine arbitrary patterns written in parallel in PMMA and developed.

One witnesses the true power of the array of zone plates when one realizes that each fires and writes its arbitrary geometry *simultaneously*. Depicted in Figure 17, an array of 3 by 3 zone plates has exposed a corresponding 3 by 3 array of unique features. The same positions in each cell are exposed together, so the full patterns are only ready at the end. If true multiplexing were implemented, each cell would contain a different pattern which would merge with its neighbors at the end of the exposure sequence to complete the die pattern.

5 Future Focus of ZPAL

5.1 Design of an Ideal ZPAL System

Looking into the future, the goals of ZPAL necessitate the development of a system that achieves the dreamed of resolution and throughput. This ideal system introduces a number of improvements or modifications to the DUV study that must undergo careful design. Evaluating the components, the radiation source changes to an x-ray undulator, the zone plates are fabricated on stiff membranes, an upstream advanced micromechanical array performs multiplexing, and the housing for the components can be under vacuum. Whether the multiplexing array will use grazing incidence mirrors or shuttering technology remains an open question.

To meet the obligations of source coherence and intensity, an undulator should be used. Although expensive, a microundulator with a 2% bandwidth (with 1 / BW magnetic sections and allowing for 50 zones) is available commercially for installation on a compact synchrotron [12]. The 4.5 nm photon will be the x-ray of choice due to its lack of proximity effect in exposing resists such as PMMA. Caution should be taken to expand the x-ray illumination via mirrors to shine on the entire zone plate array, as necessary. A calculation of the ideal ZPAL throughput using this source yields a speed of $1 \text{ cm}^2 / \text{s}$ [1].

One of the major shifts in design appears in the reconsideration of the zone plate focusing and efficiency properties. To begin, since the x-ray wavelength is so short, the zone plates need only operate with low numerical aperture, implying use of the small angle approximation. Assuming the validity of the grating equation for the outer zones $\sin \theta = \lambda / p$ and equating this

to $\tan \theta = R_N / f$, and then substituting into Equation 1 yields radically simplified expressions for the zone plate radius, focal length, and depth of focus:

$$R_N = N \cdot p, f = \frac{N \cdot p^2}{\lambda}, DoF = \frac{p^2}{2\lambda} \quad (\text{Equation 8})$$

Still, one must tackle the problem that to keep the contrast high, the high efficiency of the phase zone plate strategy is desired; indeed, in the soft x-ray regime the few available phase shifting materials also attenuate. A compromise must be reached which gives the thickness (equivalently phase shift, $\Delta\phi$) of the attenuating, phase shifting material that maximizes the contrast.

Assuming an incident flux I_i , complex refractive index $n = 1 - \delta - i\beta$, and $\eta = \beta/\delta$, the efficiencies of the m^{th} and zeroth diffracted orders are respectively [4]:

$$\frac{I_m}{I_i} = \frac{1}{m^2} \cdot \frac{1}{\pi^2} \cdot [1 + e^{-2\eta\Delta\phi} - (2 \cos \Delta\phi \cdot e^{-\eta\Delta\phi})] \quad (\text{Equation 9})$$

$$\frac{I_0}{I_i} = \frac{1}{4} \cdot [1 + e^{-2\eta\Delta\phi} + (2 \cos \Delta\phi \cdot e^{-\eta\Delta\phi})] \quad (\text{Equation 10})$$

Taking uranium as the example element, a plot of first order efficiency at $\lambda = 4.5$ nm [1] gives an acceptable peak of 31%. Finally, to explore the possible enhancements of ZPAL, one could run simulations of x-ray propagation [13] through zone plates.

5.2 Developing X-Ray ZPAL

Acknowledging the stated design rules for ZPAL using x-rays, new fabrication procedures and optics configurations arise. In particular, existing x-ray mask technology and the DUV feasibility apparatus serve as starting points to physically construct the ideal system.

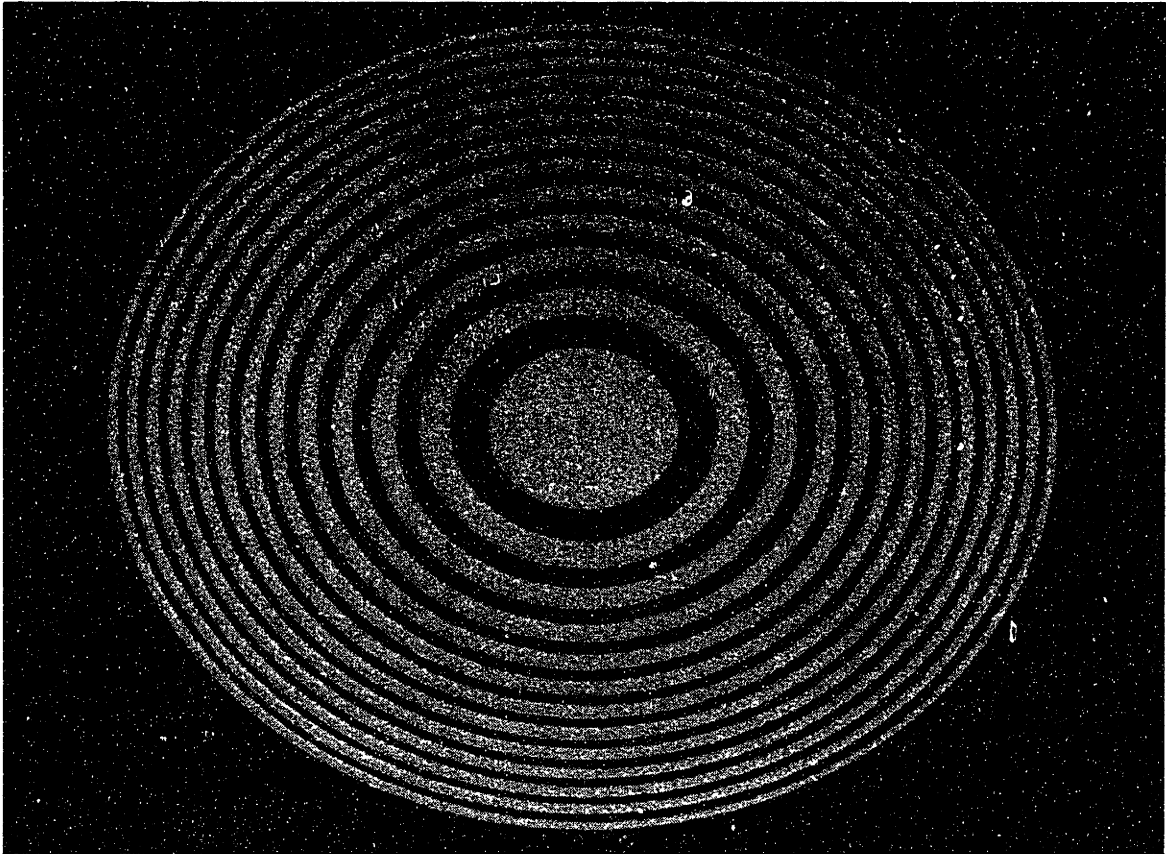


Figure 18: Scanning electron micrograph of an x-ray amplitude zone plate with 25 zones and 400 nm outer zone period. The odd zones have been gold plated on the membrane.

First of all, it should be noted that x-ray zone plates with ~30 nm resolutions have been employed in imaging for many years [14]; hence, their fabrication does not present a barrier. A common membrane made of silicon nitride provides durability. A sharp beamed SPLEBL system could generate the appropriate features without alignment error. Figure 18 displays an amplitude zone plate on a SiN_x membrane with odd zones made of gold absorber. The challenge of processing uranium for the zones lies in reactively etching through a 130 nm thickness and extraction of the volatile UF₆ species.

Building the ideal ZPAL system follows the general model of the DUV case with certain component differences. Since the undulator beamline remains in vacuum, and to prevent x-ray attenuation in gas, a chambered vacuum housing covering the multiplexing array, zone plates, and substrate stage is desirable. Also, the alignment interferometry can be directed through a window into the chamber.

5.3 Conclusions

In summary of the initial development of ZPAL done for the thesis, a review of the foreseeable benefits of this technique is presented followed by discussions of the ramifications of the DUV feasibility experiment, the obstacles to overcome, and future research into the ideal system. As a maskless lithography strategy, ZPAL stands alone in its ability to offer exceptional resolution with rapid digital patterning of arbitrary geometries. Furthermore, the simplicity of system design ensures a reliable setup.

The experimental development of ZPAL in the deep UV has broadened the vision of the system's potential [15]. The strategy for maskless lithography has been revisited and verified. Fabrication technology for processing the required nanostructures was selected and demonstrated. An apparatus to align and expose a sample using a zone plate array produced shapes. Assuming sufficient illumination, theoretical throughput computations yield an entire cell exposure in about a second. We seem well on the way to reaching the ZPAL paradigm.

Of course, certain downsides exist in the realistic implementation of ideal ZPAL on a commercial basis. The engineering hurdles experienced at this time include 1) cost effective maintenance of an undulator x-ray source, 2) fabrication of a large array of matched, equivalent zone plates with reasonable center-to-center spacing accuracy, 3) development of a

micromechanical multiplexing array structure, and 4) coordination of the multiplexing and stage control for seamless exposure.

Thus, the future focus of ZPAL research has plenty to occupy itself with, with the ultimate realization of enabling nanotechnology as its goal. Multiplexing should be demonstrated on the UV ZPAL system, probably using a micromirror array. Showing the resolution capability of the zone plates designed for the 4.5 nm x-ray wavelength would prove instrumental. Finally, combining these two paths into a functioning setup using an undulator and then even fabricating devices would challenge ZPAL to fulfill its destiny.

Appendix

```
/* C program to size the zone plates and output pattern files */

#include <stdio.h>
#include <stdlib.h>
#include <math.h>

float Radius(int n, float la, float f) {
    return sqrt(n * la * f + n*n * la*la / 4);
}

int main(void) {
    float la, zw;
    int N, ok;
    float flo, fhi, foc, dw;
    float f, RN, dof;
    int n, x, y, dx, dy, sc;
    float bias, dose, field, r1, r2;
    FILE *fzpp, *fapp;

    printf("Create .pat of Zone Plate.\n\n");
    printf("Input wavelength lambda(nm)? ");
    scanf("%f", &la);
    printf("\n");
    for (ok = 0; !ok;) {
        printf("Input outer zone width(nm)? ");
        scanf("%f", &zw);
        printf("Input number of zones N? ");
        scanf("%d", &N);
        flo = 0;
        fhi = 10000000;
        for (dw = 0; fabs(zw - dw) > .01;) {
            foc = (flo + fhi) / 2;
            dw = Radius(N, la, foc) - Radius(N-1, la, foc);
            if (dw < zw) flo = foc; else fhi = foc;
        }
        f = foc/1000;
        RN = Radius(N, la, f*1000)/1000;
        dof = .5 * la * (f/RN)*(f/RN) * (1 + N*la*.5/(f*1000));
        printf("f = %f um, RN = %f um, dof = %f nm\n\n", f, RN, dof);
        printf("Is this ok? ");
    }
}
```

```

scanf("%d", &ok);
printf("\n");
}

printf("Input field size(um)? ");
scanf("%f", &field);
fzpp = fopen("zp.pat", "w");
fprintf(fzpp, "Zone Plate la = %.1f nm, zw = %.1f nm, N = %d\n", la, zw, N);
sc = 52;
bias = 50 / 2;
for (n = 1; n < N; n += 2) {
    dose = 1.0;
    r1 = (16384/field) * (Radius(n, la, f*1000) + bias)/1000;
    r2 = (16384/field) * (Radius(n+1, la, f*1000) - bias)/1000;
    y = r1;
    dy = r2; dy = dy - y + 8192;
    x = 0;
    dx = 16383;
    fprintf(fzpp, "%d %d %d %d %d 1 0 0 %.1fn", x, y, dx, dy, sc, dose);
}
fclose(fzpp);

fapp = fopen("ap.pat", "w");
fprintf(fzpp, "Align ZP la = %.1f nm, zw = %.1f nm, N = %d\n", la, zw, N);
dose = 1.0;
r2 = (16384/field) * (Radius(N, la, f*1000) - bias)/1000;
y = 0;
dy = r2; dy = dy - y + 8192;
x = 0;
dx = 16383;
fprintf(fapp, "%d %d %d %d %d 1 0 0 %.1fn", x, y, dx, dy, sc, dose);
sc = 26;
dose = 2.0;
dx = 163;
dy = 163;
for (n = 0; n <= 3; n++) {
    if (n & 0x1) x = 15975; else x = 245;
    if (n & 0x2) y = 15975; else y = 245;
    fprintf(fapp, "%d %d %d %d %d 1 0 0 %.1fn", x, y, dx, dy, sc, dose);
}
fclose(fapp);

return 0;
}

```

References

- [1] H. I. Smith, "A proposal for maskless, zone-plate-array nanolithography", *J. Vac. Sci. Technol. B* 14, 4318 (1996)
- [2] N. M. Ceglio and H. I. Smith, *Rev. Sci. Instr.* 49, 15 (1978)
- [3] J. H. Twywissen, et al., "Nanofabrication using neutral atomic beams", *J. Vac. Sci. Technol. B* 15, 2093 (1997)
- [4] A. G. Michette, Optical Systems for Soft X-Rays, Plenum Press (1986)
- [5] H. I. Smith, Submicron- and Nanometer-Structures Technology, (1994)
- [6] J. Goodberlet, J. Ferrera, and H. I. Smith, "Spatial-phase-locked electron-beam lithography with a delay-locked loop", *J. Vac. Sci. Technol. B* 15, 2293 (1997)
- [7] J. I. Goldstein, et al., Scanning Electron Microscopy and X-Ray Microanalysis, Plenum Press (1981)
- [8] E. Hecht, Optics, Addison-Wesley Publishing (1987)
- [9] R. Loudon, Quantum Theory of Light, Oxford University Press (1983)
- [10] J. M. Florence and L. A. Yoder, "Display system architectures for digital micromirror device (DMD) based projectors", *Photonics West '96, Proc. SPIE*, vol. 2650, p. 193-208, San Jose, CA, Jan 1996
- [11] J. B. Sampsell, "Digital micromirror device and its application to projection displays", *J. Vac. Sci. Technol. B* 12, 3242 (1994)
- [12] Aurora 2D, Sumitomo Heavy Industries, Ltd., Tokyo, Japan, and communication E. Toyota of Sumitomo Heavy Industries
- [13] S. D. Hector, et al., "Modeling and experimental verification of illumination and diffraction effects on image quality in x-ray lithography", *J. Vac. Sci. Technol. B* 10, 3164 (1992)
- [14] G. Schmahl, et al., *Optik* 93, 95 (1993)
- [15] I. J. Djomehri, T. A. Savas, and H. I. Smith, "Zone-plate-array lithography in the deep UV", To be published *J. Vac. Sci. Technol. B*, Nov/Dec 1998

THESIS PROCESSING SLIP

FIXED FIELD: ill. _____ name _____
index _____ biblio _____

► COPIES: Archives Aero Dewey Eng Hum
Lindgren Music Rotch Science

TITLE VARIES: ► _____

NAME VARIES: ► _____

IMPRINT: (COPYRIGHT) _____

► COLLATION: 47 p

► ADD: DEGREE: _____ ► DEPT.: _____

SUPERVISORS: _____

NOTES:

cat'r:	date:
► DEPT: <u>E.E.</u>	page: <u>532</u>
► YEAR: <u>1998</u>	► DEGREE: <u>S.M.</u>
► NAME: <u>DJOMEHRI, Ihsan Jahed</u>	